Tuning physical properties of $NiFe_2O_4$ and $NiFe_2O_4$ coated with SiO_2 nanoparticles by thermal treatment

S. Lewińska[a], A. Bajorek[b,c], C. Berger[d], M. Dulski[c,e], M. Zubko[c,e], K. Prusik[c,e], A. Ślawska-Waniewska[a], F. Grasset[f], N. Randrianantoandro[g]

[a] Institute of Physics, Polish Academy of Sciences, Warsaw, Poland; [b] A. Chełkowski Institute of Physics, University of Silesia in Katowice, 75 Pułku Piechoty 1, 41-500 Chorzów, Poland, [c] Silesian Center for Education and Interdisciplinary Research, University of Silesia in Katowice, 75 Pułku Piechoty 1A, 41-500 Chorzów, Poland, [d] Université François-Rabelais, Greman, UMR 7347, 16 rue Pierre et Marie Curie, 31071 Tours, France, [e] Institute of Materials Science, University of Silesia in Katowice, 75 Pułku Piechoty 1A, 41-500 Chorzów, Poland, [f] Univ Rennes, CNRS, ISCR (Institut des Sciences Chimiques de Rennes) – UMR 6226, 35000 Rennes, France, [g] l'Institut des Molécules et Matériaux du Mans UMR CNRS 6283, Le Mans Université, Avenue Olivier Messiaen, 72085 Le Mans, Cedex 9, France.

To read more: Bajorek, A., et al. Tuning Physical Properties of $NiFe_2O_4$ and $NiFe_2O_4@SiO_2$ Nanoferrites by Thermal Treatment. Metall Mater Trans A 53, 1208–1230 (2022). https://doi.org/10.1007/s11661-021-06567-0

Summary

The comparison between $NiFe_2O_4$ (co-precipitation) and $NiFe_2O_4$ coated with SiO_2 (co-precipitation and microemulsion) ferrite nanoparticles in their as-received and annealed form is presented. The structural characterization revealed the gradual crystallization of as-received samples induced by thermal treatment. The existence of cubic inverse spinel ferrite structure with tetrahedral and octahedral iron occupancy is confirmed in all samples by the comprehensive study. In the case of nanoparticles embedded into the silica matrix, the crystallization of initially amorphous silica is revealed in structural and microstructural characterization. The separation of the rhombohedral hematite α-Fe_2O_3 phase in the $NiFe_2O_4$ ferrite evidenced during the annealing process is demonstrated in structural and magnetic studies. The room temperature superparamagnetic state (SPM) is modified in the $NiFe_2O_4$ sample by annealing as an effect of ferrite crystallization and grain growth as well as hematite separation. For as-received $NiFe_2O_4$, with temperature decrease, the blocking process preceded by the freezing process is observed. The silica shell is recognized as the sustaining cover for the SPMstate. The electronic structure studies confirmed the complex nature of the Fe-based states.

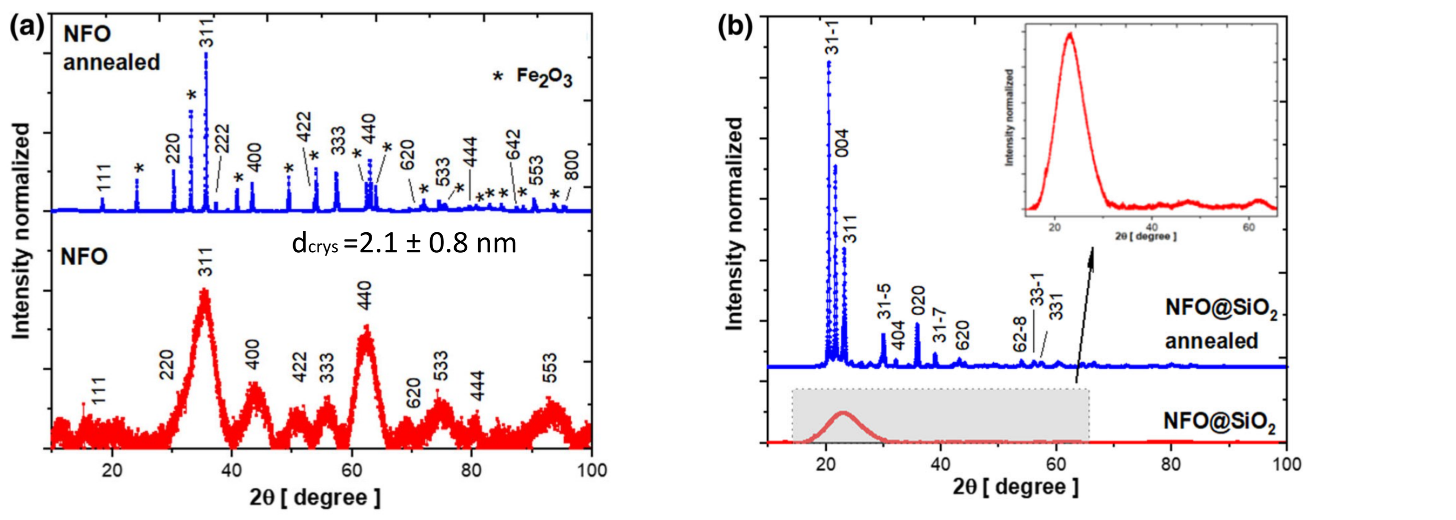

Fig. 1. XRD patterns for the investigated samples.

$NiFe_2O_4$

- cubic inverse spinel structure (*Fd3-m*) , d ~ 2 nm
- the diffraction peaks are broadened, indicating the ultrafine crystal structure

$NiFe_2O_4$ annealed

- 52% $NiFe_2O_4$ → cubic inverse spinel structure (*Fd3-m*) d ~ 58 nm
- 48% rhombohedral hematite α-Fe_2O_3 (*R-3c*) d ~ 91 nm

$NiFe_2O_4$ coated with SiO_2

- spectrum dominated by the broad peak → tetragonal SiO_2 structure (amorphous silica matrix)
- trace of crystalline $NiFe_2O_4$ nanoparticles covered by SiO_2

$NiFe_2O_4$ coated with SiO_2 annealed

- SiO_2 crystallized in the monoclinic *Aa* structure (d ~ 77 nm)
- no evidence of $NiFe_2O_4$

$NiFe_2O_4$ / $NiFe_2O_4$ coated with SiO_2

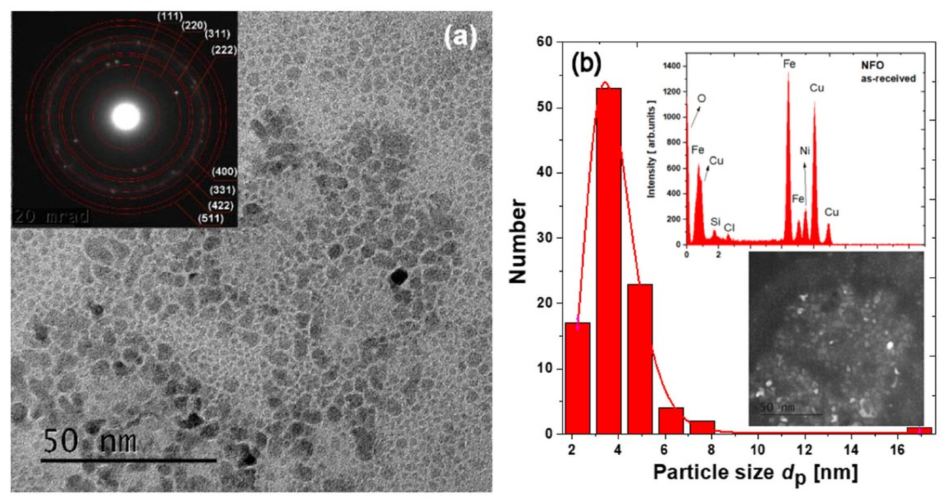

Fig 2. (a) TEM micrograph and the SAED pattern for $NiFe_2O_4$
→ randomly oriented polycrystalline grains with inverse spinel symmetry .
(b) Crystallite size distribution, and EDS analysis → d ≈ (3.7 ± 0.3) nm. The EDS spectrum confirmed the presence of the $NiFe_2O_4$ phase.

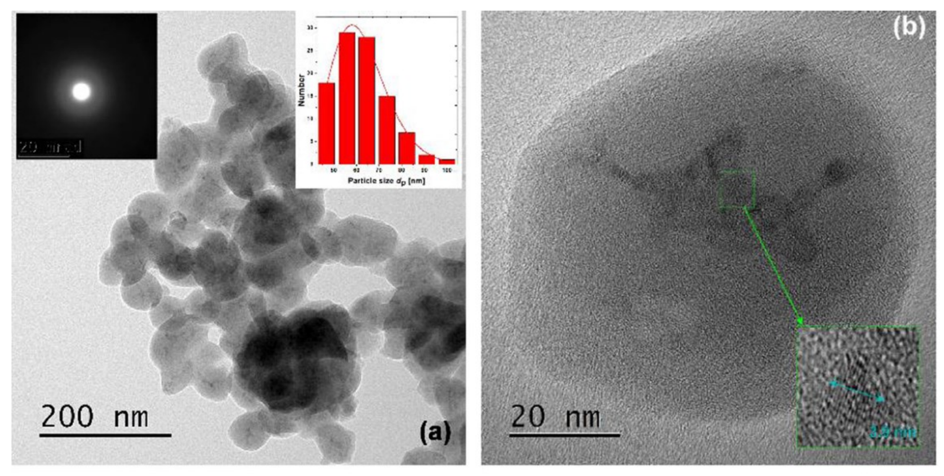

Fig 3. (a) TEM micrograph and the SAED pattern for $NiFe_2O_4$ coated with SiO_2
→ particles are almost spherical, d ~ 60 nm.
(b) The HR-TEM image → irregular distribution of $NiFe_2O_4$ inside SiO_2.

$NiFe_2O_4$ annealed / $NiFe_2O_4$ coated with SiO_2 annealed

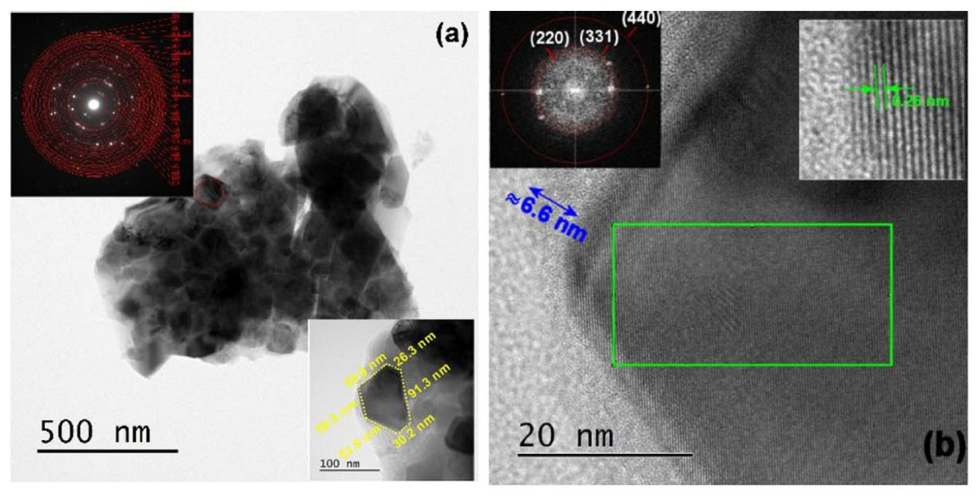

Fig 4. (a) TEM micrograph and the SAED pattern for the annealed $NiFe_2O_4$ nanoparticles → well-crystallized nanoparticles, d ~ 72 nm, polygon shape.
(b) The HR-TEM image of one crystallite → interplanar spacing of 0.26 nm between adjacent planes, corresponding to (311) $NiFe_2O_4$ lattice plane.

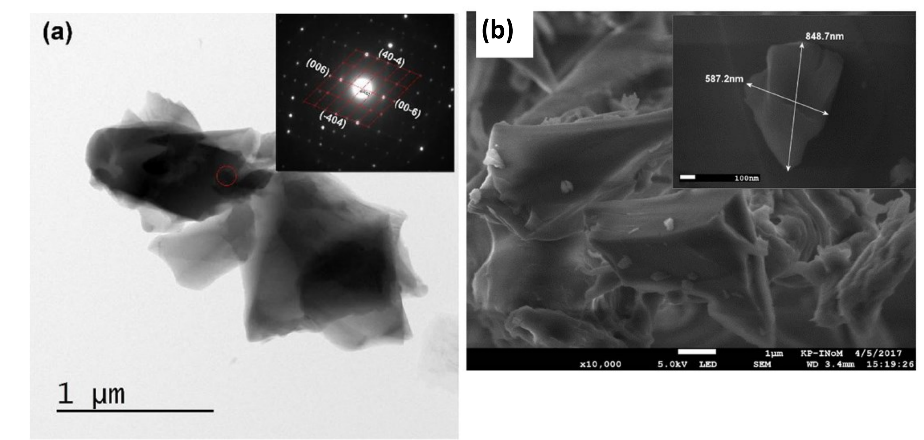

Fig 5. (a) TEM micrograph and the SAED pattern for the annealed $NiFe_2O_4$ coated with SiO_2 → spherically shaped particles disappeared; thin irregular flakes (crystallized SiO_2) have emerged.
(b) The SEM image → large irregular grains, size ~ 600 nm.

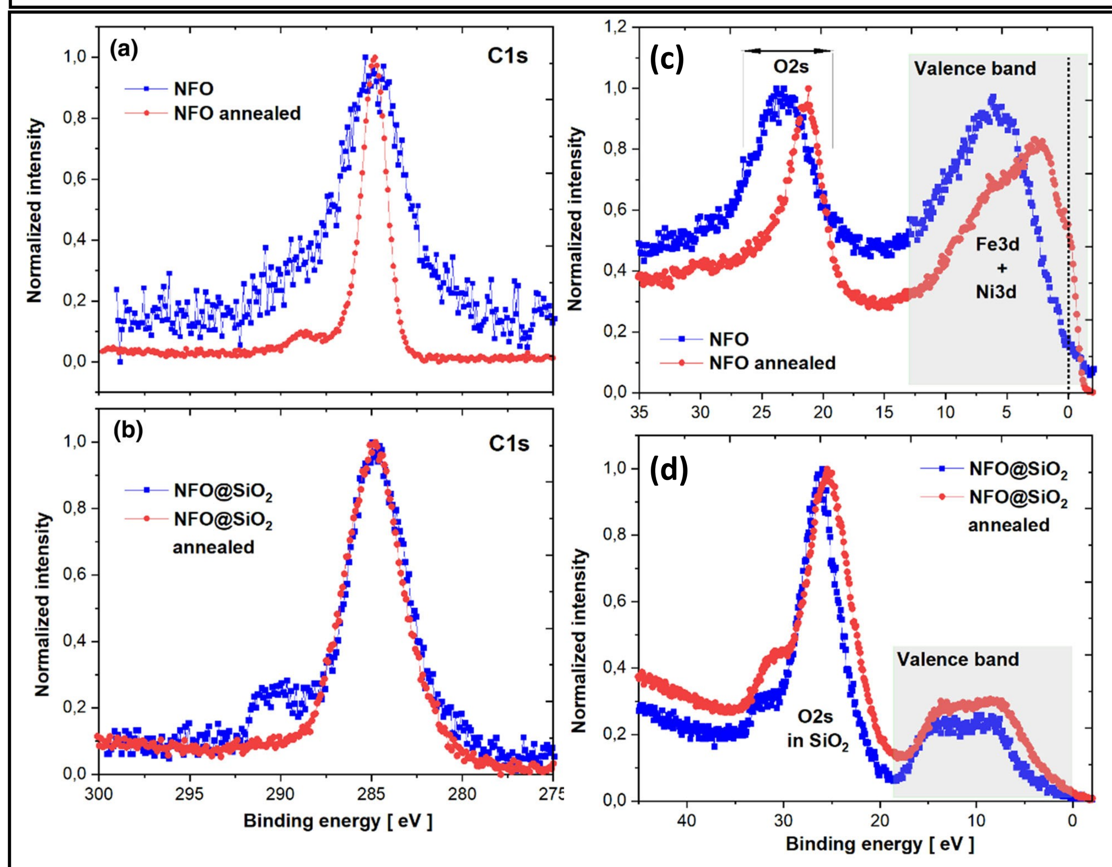

C1s states
- carbon line (impurity on the surface) at 284.8eV
- low-intensity separate peak at about 288.7 eV (overlapped states from carbonyl (C=O) and carboxyl (O=C–OH) groups)

O2s states
- moved towards the lower binding energy range after annealing

Ni3d/Fe3d states
- for $NiFe_2O_4$ hybridized states dominated at the Fermi level (shape of VB)
- for coated samples, broad band peaking around 13.2 and 8.5 eV are dominated by hybridized O2p, Ni3d/Fe3d states and low-intensity Si3p/s states

Fig. 6. Comparison between C1s states (a) - (b), and between valence bands spectra (c) - (d).

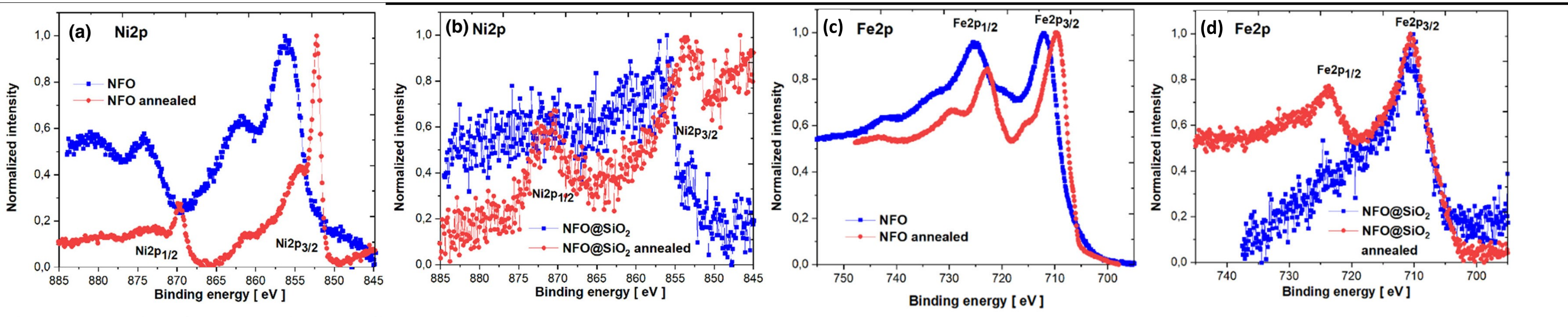

Fig. 7. Comparison between Ni2p Fe2p lines.

$NiFe_2O_4$
two binding energy peaks: 854.7 eV ($Ni2p_{3/2}$), 871.8 eV ($Ni2p_{1/2}$)
broad satellite peaks: ~ 862 eV and 879 eV

$NiFe_2O_4$ annealed
$Ni2p_{3/2}$ → metallic Ni line (852.4 eV) 16.2 %, spinel ferrite line (854.3 eV) 31.2%,

$NiFe_2O_4$ coated with SiO_2
Ni line barely visible → position similar to $NiFe_2O_4$

$NiFe_2O_4$ coated with SiO_2 annealed
$Ni2p_{3/2}$ → metallic Ni line (852.2 eV) 23.44 %, spinel ferrite line (853.7 eV) 40.72 %, 6eV satellites structure (855.28 and 856.36 eV)

$NiFe_2O_4$
$Fe2p_{3/2}$ and $Fe2p_{1/2}$ lines + satellites at 719.2 and 733.5 eV confirming the existence of Fe^{3+} ions

$NiFe_2O_4$ annealed
lines are shifted towards a lower binding energy iron species exist in more than one chemical state (metallic Fe, and Fe_2O_3)

$NiFe_2O_4$ coated with SiO_2
weak Fe2p line

$NiFe_2O_4$ coated with SiO_2 annealed
typical inverse spinel ferrite structure with the ratio of $Fe^{3+}(A)/Fe^{3+}(B)$ ≈ 0.8 and about 21.9 % contribution of metallic iron

Temperature dependences of the magnetization (VSM measurements)

→ zero field cooled - field cooled regime

→ H_{ext} = 100 Oe, 1000 Oe

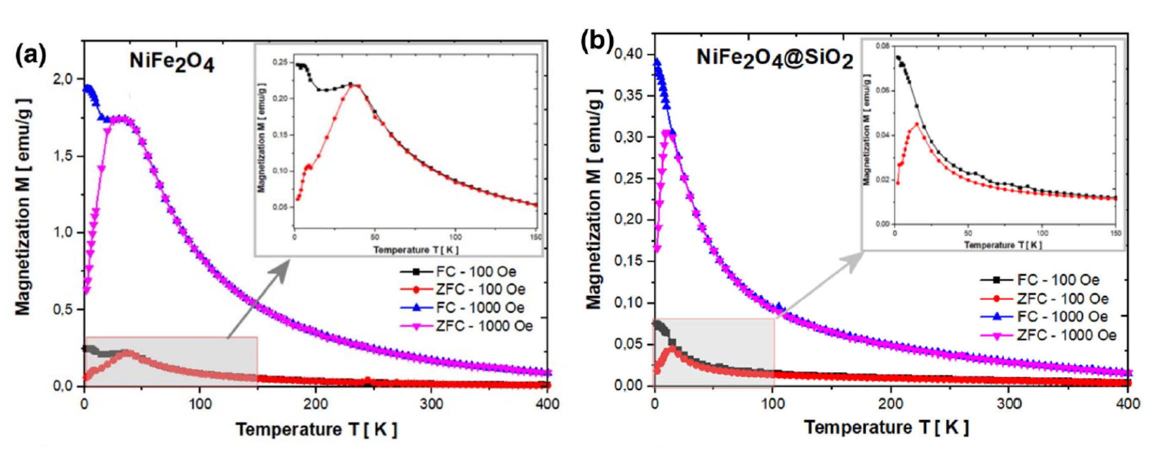

Fig. 8. ZFC-FC curves for the as-received samples.

$NiFe_2O_4$

- two maxima: T_{max1} ~ 32 K, and T_{max2} ~ 7 K → the freezing process is observed before the blocking process
- the reversibility of ZFC-FC curves from T_{max1} to 400 K → superparamagnetic behavior

$NiFe_2O_4$ coated with SiO_2

- the ZFC maximum at T_{max} ≈ 14.8 K (100 Oe) and ≈ 11.9 K (1000 Oe) → blocking process
- $NiFe_2O_4$ particles are well dispersed in the silica matrix → the interaction between them is negligible

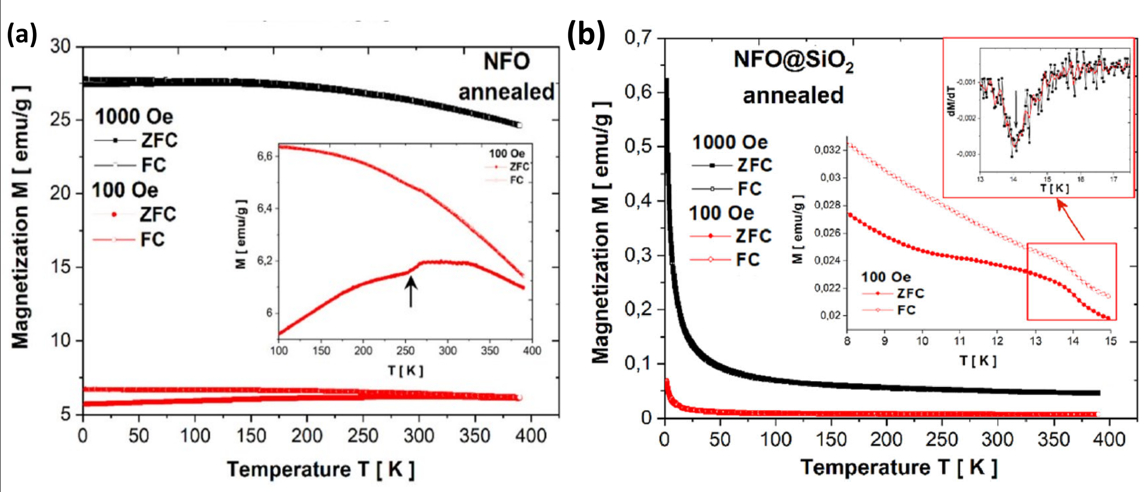

Fig. 9. ZFC-FC curves for the annealed samples.

$NiFe_2O_4$ annealed

- blocking or freezing processes are excluded → system behaves as a bulk material
- a kink in the ZFC curve between 250 K and 260 K denotes the Morin transition

$NiFe_2O_4$ coated with SiO_2 annealed

- ZFC and FC curves show the magnetization increases with decreasing the temperature as in the paramagnetic system → the decomposition of ferrite nanoparticles to paramagnetic ions due to the annealing process
- a broad maximum ~ 14 K → residues of ferrite nanoparticles

Magnetization curves (VSM measurements)

→ field range ± 90 kOe

→ T = 2 K, 100 K, 300 K

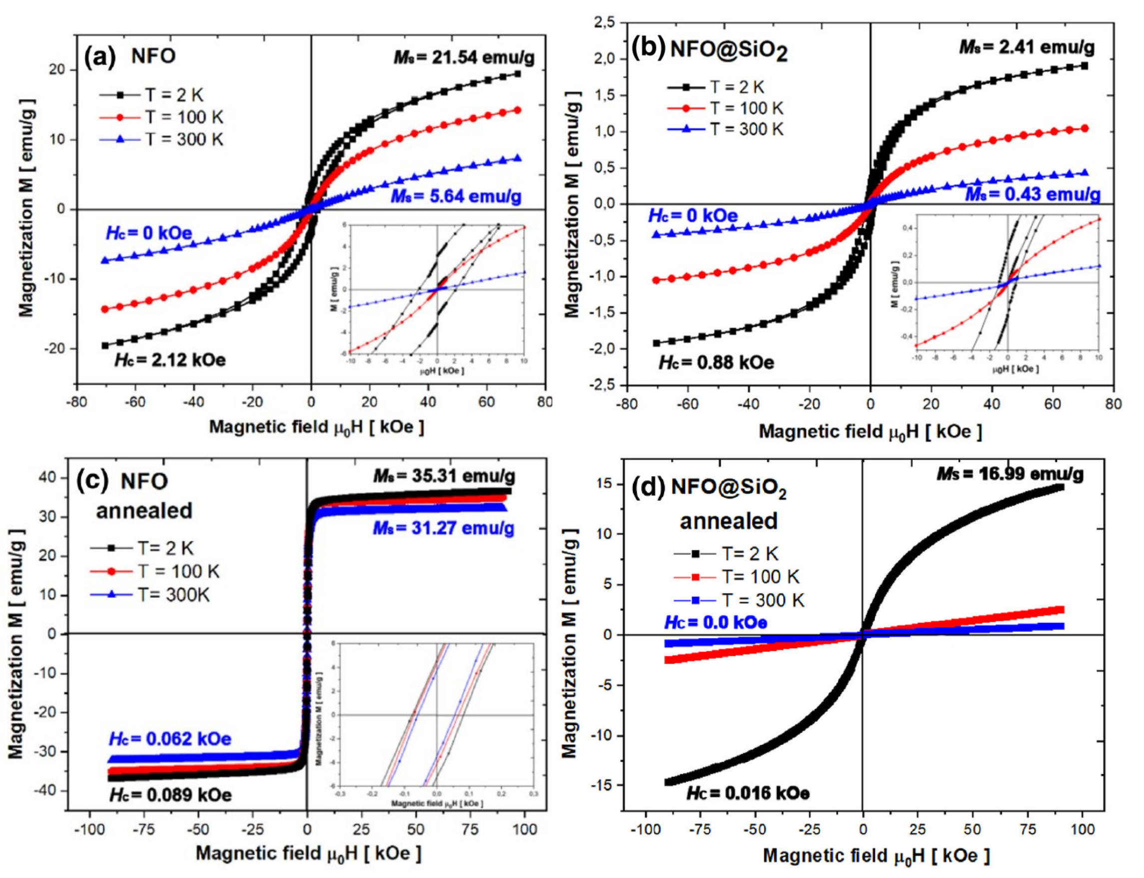

Fig. 10. M(H) curves for the investigated samples.

Anisotropy

$$M(H) = M_S\left(1 - \frac{a}{\sqrt{H}} - \frac{b}{H^2}\right) + \chi_p H$$

$$b \approx \frac{8}{105}\left(\frac{K_1}{\mu_o M_S}\right)^2$$

K_1 [10^5 erg/cm^3]	T= 2K	T= 100 K	T= 300 K
$NiFe_2O_4$	3.51	2.93	1.32
$NiFe_2O_4$ coated with SiO_2	0.36	0.25	0.09
$NiFe_2O_4$ annealed	0.97	1.95	1.17
$NiFe_2O_4$ coated with SiO_2 annealed	3.79	-	-

K_1 is reduced with the increase of particle size

crystallization of silica shell and subsequent modification of $NiFe_2O_4$ particle coating

Mössbauer spectra

→ T = 77 K, 300 K

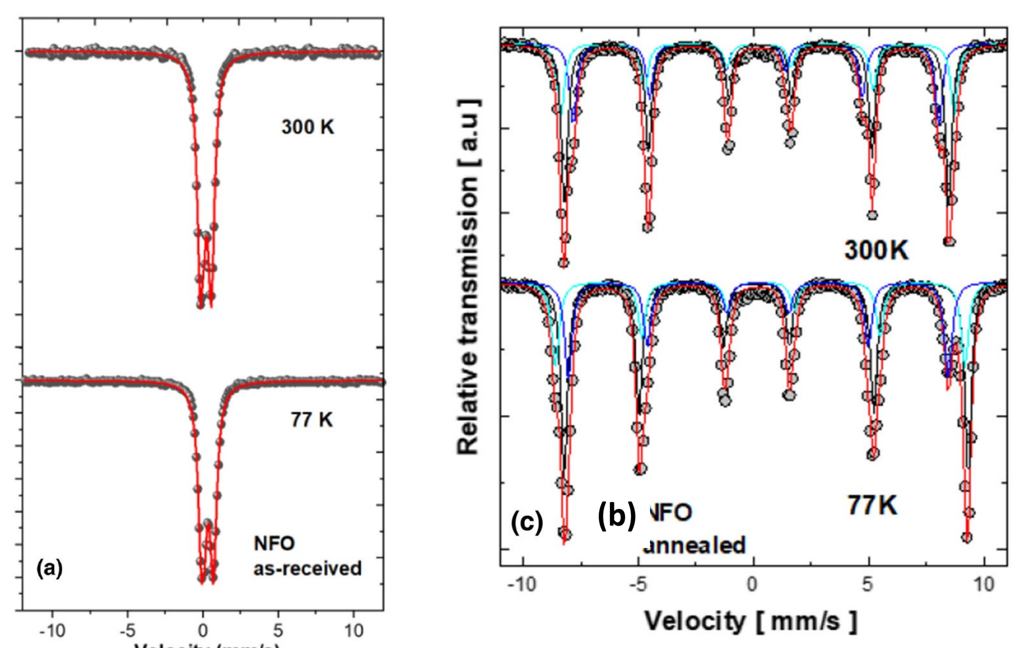

Fig. 11. Mössbauer spectra for $NiFe_2O_4$ (a) and $NiFe_2O_4$ annealed (b). The results for the samples coated with silicon are similiar to (a).

		IS (mm/s)	QS/2ε (mm/s)	B_{hyp} (T)	FWHM/2 (mm/s)	A (%)	Phase
$NiFe_2O_4$							
T = 300 K		0.32	0.63	-	0.26	100	$NiFe_2O_4$
T = 77 K		0.44	0.67	-	0.27	100	$NiFe_2O_4$
$NiFe_2O_4$ coated with SiO_2							
T = 300 K		0.33	0.65	-	0.25	100	$NiFe_2O_4$
T = 77 K		0.43	0.63	-	0.26	100	$NiFe_2O_4$
$NiFe_2O_4$ annealed							
T = 300 K	Site A	0.26	0	49.0	0.18	27	$NiFe_2O_4$
	Site B	0.36	-0.05	52.7	0.18	24	$NiFe_2O_4$
		0.37	-0.16	51.5	0.16	49	α-Fe_2O_3
T = 77 K	Site A	0.36	0.02	50.9	0.19	24	$NiFe_2O_4$
	Site B	0.46	-0.04	54.9	0.19	28	$NiFe_2O_4$
		0.50	0.42	54.1	0.17	48	α-Fe_2O_3
$NiFe_2O_4$ coated with SiO_2 annealed							
T = 300 K		0.26	0.83	-	0.29	100	$NiFe_2O_4$
T = 77 K		0.37	0.88	-	0.32	100	$NiFe_2O_4$